SCIENCE CHINA
Information Sciences

• **Supplementary File** •

An Aircraft Conflict Resolution Method Based on Hybrid Ant Colony Optimization and Artificial Potential Field

Huaxian LIU[1,2], Feng LIU[1,2], Xuejun ZHANG[1,2*], Xiangmin GUAN[3], Jun CHEN[4] & Pascal SAVINAUD[5]

[1]*School of Electronic and Information Engineering, Beihang University, Beijing, 100191, China;*
[2]*National Key laboratory of CNS/ATM, Beihang University, Beijing, 100191, China;*
[3]*Department of General Aviation, Civil Aviation Management Institute of China, Beijing 100102, PR China;*
[4]*Queen Mary University of London, London, UK;*
[5]*Direction des Services de la Navigation Arienne (DSNA), Reims, France*

Appendix A Conflict Detection

As shown in Figure A1, the flight trajectories of mathematical modeling in subsequent time T_w can be predicted and the distance d(t)(i, j) between two aircraft at time t can be described as follows:

$$d(t)(i,j) = \sqrt{(x_i(t) - x_j(t))^2 + (y_i(t) - y_j(t))^2} t \in [0, T_w] \tag{A1}$$

If the minimum distance between two aircraft $d_{min}\,(i,j)$ within the time T_w is less than the safety separation distance, i.e. $d_{min}\,(i,j) < d_{safe}$, then a conflict is considered. The safety separation d_{safe} is 5 nautical miles (NM) according to the ICAO (International Civil Aviation Organization) Doc 4444 [ref].

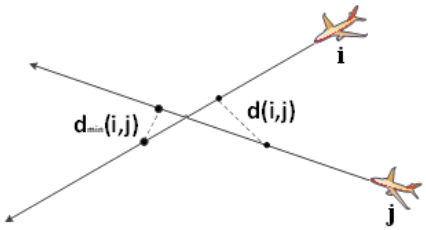

Figure A1 An example of aircraft conflict

The conflict detection method adopted in this paper is depicted in Figure A2.
The positions of flight 1 and 2 can be worked out using equations A2) and A3).

$$(x_1', y_1') = (x_1 + vt\cos\theta_1, y_1 + vt\sin\theta_1) \tag{A2}$$

$$(x_2', y_2') = (x_2 + vt\cos\theta_2, y_2 + vt\sin\theta_2) \tag{A3}$$

Substitute equation A2) and A3) into equation A1) and take differentiation with respect to t,$d\,(t)\,(1,2)\,/dt = 0$is obtained. We can get the time t_{min} when the distance is minimum of the two aircraft.

$$t_{\min} = \frac{(x_2 - x_1)(\cos\theta_2 - \cos\theta_1)}{2v[\cos(\theta_2 - \theta_1) - 1]} + \frac{(y_2 - y_1)(\sin\theta_2 - \sin\theta_1)}{2v[\cos(\theta_2 - \theta_1) - 1]} \tag{A4}$$

Figure A3 shows that when a conflict happens, an effective and ideal trajectory is urgently needed to avoid collision and maintain the safety distance between aircraft by changing their heading, speed or altitude.More specifically, this means that for any $t \in [0, Tw]\,, d\,(t)\,(i,j) > d_{safe}$.

* Corresponding author (email: zhxj@buaa.edu.cn)

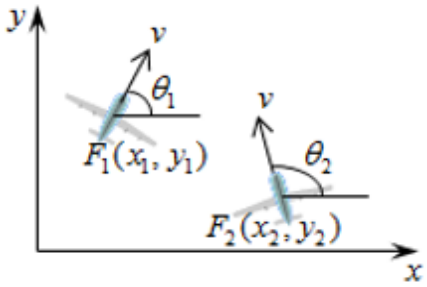

Figure A2 Conflict detection

Figure A3 An example of aircraft conflict resolution

Appendix B Conflict Resolution based on Artificial Potential Field Method

The conflict resolution problem is turned into a physics problem by creating an electric field of positive and negative charges. The main idea is to establish the potential and vortex fields, where the destination is the positive charge, and all aircraft are the negative charges. Therefore, charges in different polarity attract each other to ensure that every aircraft will reach the destination. Aircraft will repel each other as they are in the same polarity and this will avoid conflict.

The trajectory of each aircraft is then determined by the force analysis. Specifically, suppose there are n aircraft, the position of the i-th aircraft is $\vec{x}_i = (x_i, y_i)$. The method is illustrated using an example of two aircraft i and j shown in Figure B1.

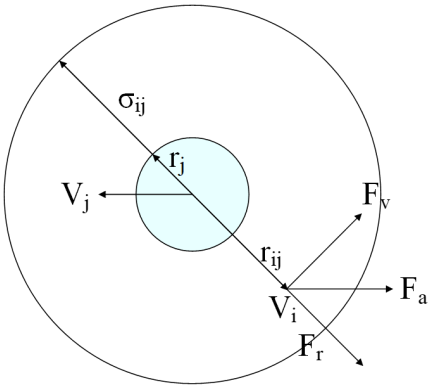

Figure B1 Illustration of the artificial potential field between aircraft i and j

In order to make sure the aircraft flying to a specified destination, the destination $\vec{x}_{di} = (x_{di}, y_{di})$ is the potential field, which is given by the attractive potential function:

$$U_a(\vec{x}_i, \vec{x}_{di}) = \frac{1}{2}(\vec{x}_{di} - \vec{x}_i)^2 \tag{B1}$$

The destination will generate the attractive force which is defined by:

$$F_a(\vec{x}_i, \vec{x}_{di}) = -\nabla U_a(\vec{x}_i, \vec{x}_{di}) = -(\vec{x}_i - \vec{x}_{di}) \tag{B2}$$

where Fa is the force proportional to the negative gradient of U_a.

To avoid a collision, the j-th aircraft will construct a spherically symmetric repulsion field:

$$U_r(x_i, x_j) = \begin{cases} -\frac{(r_{ij} - (r_j + \sigma_{rj}))^2}{2\sigma_{rj}} & r_j \leqslant r_{ij} \leqslant r_j + \sigma_{rj} \\ 0 & otherwise \end{cases} \tag{B3}$$

where $r_{ij} = \sqrt{(x_i - x_j)^2 + (y_i - y_j)^2}$ is the distance between the i-th and j-th aircraft. σ_{rj} is the protection radius of the j-th aircraft which is the area where the repulsive force exists.

When the i-th aircraft entered into the repulsion field of the j-th aircraft, the repulsive force is defined by

$$F_r(x_i, x_j) = \nabla U_r(x_i, x_j) \tag{B4}$$

In order to ensure the aircraft involved in conflict follow the same resolution strategy, the vortex field is added which is tangential to the repulsion field, ensuring all aircraft turn in the same direction.

$$F_v(x_i, x_j) = \pm \begin{bmatrix} \frac{\partial U_r(x_i,x_j)}{\partial y} \\ -\frac{\partial U_r(x_i,x_j)}{\partial x} \end{bmatrix} \tag{B5}$$

With the three force fields mentioned above, we can get a dynamic path planning equation for multi-aircraft as below:

$$\dot{x}_i = \frac{F_a(x_i, x_{di})}{||F_a(x_i, x_{di})||} + \sum_j (k_{ri} F_r(x_i, x_j) + k_{vi} F_v(x_i, x_j)) \tag{B6}$$

where $j = 1, \ldots, m, i \neq j$. The repulsive and vortex fields ensure safe separation among aircraft. And the attractive filed will push aircraft to the destination. The repulsive factor k_{ri} and the vortex factor k_{vi} are used to show the influence of the repulsive and vortex forces. Converting $\dot{x}_i$ into unit vectors will get the direction of the velocity. If the speed of aircraft is k_{di}, then the velocity of aircraft will be $\overrightarrow{v_i} = k_{di} \frac{\dot{x}_i}{|\dot{x}_i|}$. Finally, we can get the conflict resolution path of multi-aircraft.

Assume that there are six aircraft uniformly distributed on a circle with the radius of 100 NM, and each aircraft flies along a straight path. Obviously, conflict will happen in the center of the circle. The trajectories obtained by the artificial potential field method are shown in Figure B2.

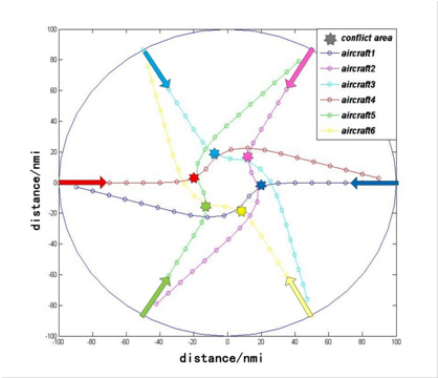

Figure B2 The results of artificial potential field method

The shortest distance between two aircraft is 12.34 NM, meeting the requirements of the 5 NM safety distance. However, it can be seen that this method can cause impractical heading change. Therefore, it is not suitable in a real-world scenario, especially when the number of aircraft increases.

Appendix C Conflict Resolution based on Ant Colony Optimization

The conflict resolution path will be discretized into K steps firstly. A_i, B_i means the i-th steps of the A and B aircraft as shown in Figure C1. Each aircraft will maintain a certain speed and direction during each step, and will change their direction before the next step.

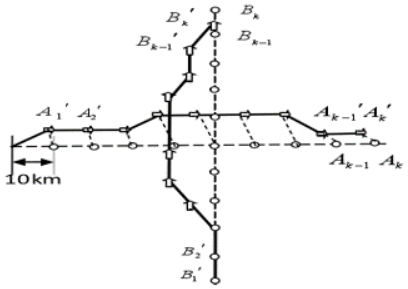

Figure C1 Discretization of conflict resolution path

Considering the feasibility of aircraft in their cruise phase, the aircraft is assumed to only choose three flight directions, including their original directions and turning 30 degrees to the right or left. This assumption reduces the search space and reduces the pilot's reaction time which makes the implementation of the conflict resolution solution easier.

In summary, assuming that there are n aircraft, each aircraft has K steps to adjust, and every step is coded into 1 (turn 30 degrees right), -1 (turn 30 degrees left), and 0 (maintain their original direction). As a result, each conflict resolution path

will be encoded as a N*K-dimensional vector $\vec{X} = (x_1, x_2, \ldots, x_{N*K})$, $x_i \in \{-110\}$. i.e. each k components correspond to a conflict resolution path of an aircraft.

As shown in Figure C2, suppose there is a 3*NK maze through which ants need to traverse to find the food. There are three nodes for ants to choose at each step. Thus, each ant foraging path represents an encoding vector described above, indicating a conflict resolution program.

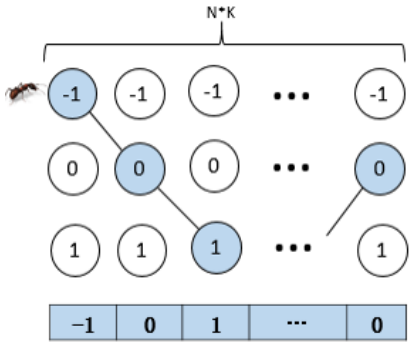

Figure C2 Encoding mechanism

Keeping safety and reducing delay are the main objectives of the CR problem. In this paper, safe separation between aircraft is included as a hard constraint, i.e. only the conflict-free solution can survive into the next generation. Hence, total delay S reduction is as the objective and defined as below.

$$\min S = \sum_{i=1}^{N} |TR_i - TP_i| \tag{C1}$$

where TR_i is the real arrived time of aircraft i and TP_i is the planned arrived time.

The same situation of eight aircraft is simulated as for the arfitifial potential field method. The results using the ant colony optimization method are shown in Figure C3.

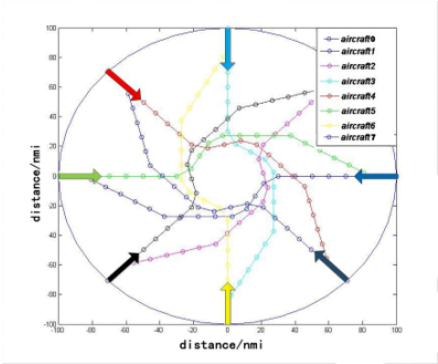

Figure C3 The results of the ant colony optimization method

As it can be seen, the shortest distance between two aircraft is 11.43 NM, meeting the requirements of the 5 NM safety distance. However, even with high performance computer, the algorithm needs about a minute to obtain all resolutions, which is too long for an online decision support tool.

Appendix C.1 Encode the results of the artificial potential field to get "authority" Ants

The heading of aircraft in the artificial potential field is decided jointly by the attraction of destination and repulsion of aircraft, which makes the heading deflection range from 0 to 180 degrees. However, in CR based on ACO, heading deflection can only take three discrete values, i.e. 0 and 30 degrees. Therefore, an appropriate approximation of the path obtained by the artificial potential field is needed.

In fact, the heading of each aircraft at each step determines the CR path. If the deviation between the original heading and the heading as a result of the artificial potential field is within an allowable range (15 degrees), aircraft will fly along the original heading. Otherwise, the heading should be adjusted. The path obtained by the artificial potential field method is shown in Figure C4, together with the adjusted path according to the aforementioned rule. The adjusted path will then be encoded as the foraging path of Authority ants.

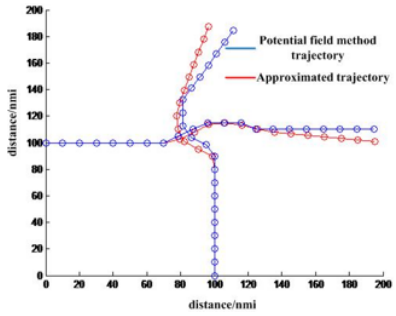

Figure C4 Path approximation

Appendix C.2 The "authority ant colony " generated by the "authority ant"

In fact, the approximated path may not be the best solution and may be significantly different from the original path. In order to avoid accidental error caused by the approximation method, The "authority ant colony" is generated by the "authority ant" using the genetic variation from the genetic algorithm [1].

Mutation operation is one of the most important steps in the genetic algorithm. During mutation, the value of some genes in the individual code string is replaced, based on the mutation probability P_m, with the value of other genes to generate a new individual code string. This is an auxiliary method to generate a new individual, which determines the local search ability of genetic algorithm and maintains the diversity of the population.

Inspired by the mutation operation, an authority ant path is obtained iteratively as $\vec{X} = (x_1, x_2, \ldots, x_{N*K})$ $x_i \in \{-110\}$ where the N*K-th component of $\vec{X}$ can be regarded as the gene for the path. Some genes are randomly selected to mutate into other possible values. Moreover, conflict checking is carried out on the new individual after the mutation. If the new solution meets the safety requirements (i.e. no flight conflict), a new "authority ant" would be generated successfully. This operation is repeated until the "authority ant colony" is obtained.

Appendix C.3 Initialization of pheromone matrix by using the "authority ant colony"

Each "authority ant" will secrete a certain degree of pheromones on its path according to the delay caused by the conflict resolution solution, and pheromones of each node on the path will be updated based on the rule below.

$$\tau_{ij}(t+1) = (1-\rho)\tau_{ij}(t) + Q/S \tag{C2}$$

where $\tau_{ij}(t)$ is the pheromone of the jth row and the ith node of the pheromone matrix. ρ is the volatile factor, ranging from 0 to 1, with respect to volatile speed of pheromones. S is the summation of all aircraft delays computed using the conflict resolution solution. As described above, the lower the S, the more pheromones will be secreted by ants. Hence, there is a negative relationship between S and pheromones. Q is the coefficient of the gain which is used to adjust the pheromones into a proper magnitude.

After updating the pheromones by the equation above in the nodes visited by the ants in the "authority ant colony", we can get the initialization of the pheromone matrix.

The ant colony optimization algorithm is then used to obtain the conflict resolution solution, taking into account all constraints.

After initialization of pheromones by the "authority ant colony", the probability of ants to select the node in the first generation is proportional to the intensity of the pheromone in the node$P_{ij} = \tau_{ij} / \sum_{i=1}^{3} \tau_{ij}$. As the "authority ant colony" is generated by the conflict resolution path obtained by the artificial potential field method, it can guide the subsequent ants to find a safe and conflict-free path according to the initialization pheromone matrix. It can avoid the problem of the ant colony optimization algorithm being randomly initialized with many invalid paths in the early stages.

As described previously, ants following an invalid path will not secrete pheromones. Therefore, only when the safety of flights is satisfied, ants will secrete pheromones on their path based on the amount of the delay. Hence, a positive feedback of pheromones is formed to accelerate convergence of the solution. The ant colony can quickly find a safe and efficient path by using the "authority ant colony" initialization pheromone matrix. A "positive feedback" process is established rapidly, which greatly speeds up the convergence rate of algorithm.

Appendix D Evaluation Index

In this paper, in order to show the effectiveness of the proposed algorithm, four main indices are employed in the conflict resolution problem. These are conflict probability, computational load, feasibility and system efficiency.

Conflict probability is an important index to evaluate safety of the conflict resolution system, and is defined as:

$$CP = \frac{\sum_{j=1}^{N} c_j}{N} \tag{D1}$$

In which c_j is the conflict number of the j-th aircraft, and N is the total number of aircraft. Average computational load of the algorithm is indicated as:

$$CL = \frac{1}{n}\sum\nolimits_{j=1}^{n} T_j \tag{D2}$$

where n is the number of repeated experiments, and T_j is the time needed for the j-th experiment. In the conflict resolution solution, some solution may violate restrictions due to physical conditions of real aircraft. Feasibility can be introduced as:

$$F = \sum\nolimits_{i=1}^{n} f_i \tag{D3}$$

where f_i is the number of infeasible points of the i-th aircraft in the conflict resolution solution. F is used to evaluate the feasibility of the conflict resolution solution. Taking the high-speed of aircraft into account, flight conflicts need to be solved in real time in order to ensure flight safety. The computational time means the time different algorithms needed to solve the problem. Hence, system efficiency of the algorithm is given by:

$$SE = \frac{1}{N} \cdot \sum_{i=1}^{N} (\frac{S_{di}}{S_i + S_{di}}) \tag{D4}$$

In which S_i is the delay of the i-th aircraft, and S_di is the planning time of the i-th aircraft. Obviously, when all aircraft are flying along the preset path, SE = 1; when the number of aircraft involved in conflict increases, SE decreases accordingly.

Appendix E Scenario description

Two typical scenarios [2–4] were used to test the proposed method as shown in Figure E1. In the classical scenario, all aircraft are uniformly distributed in a circle, the radius of the circle is 100 NM, and each aircraft flies along a straight path. Obviously, without resolution, conflict will occur in the center of the circle. Although this is an extreme scenario which is less likely to happen, it can provide insight into performance about the improved algorithm and its ability to deal with the complicated situation. Krozel et al. [3] presented the random flights scenario in 2002 which used two concentric circles. Aircraft appear randomly at the outer circle (radius 120 NM) and the destination points are assigned randomly on the inner circle (radius 100 NM). The 20NM interval between two circles prevents the initial conflict between aircraft. Because this scenario can test the efficiency of the algorithm under different circumstances, it is a good test for different conflict resolution algorithms [2].

The parameter setting is shown in the Table E1.

Table E1 Parameters of the experiments

Parameter	Artificial Potential Flgield	Genetic algorithm	Ant colony optimization	Improved algorithm
Radius of the circle	120NM		120NM	120NM
Protection radius()	10NM		10NM	10NM
Attractive parameter(A_p)	1		–	1
Repulsion parameter(R_p)	2.5		–	2.5
Vortex parameter(V_p)	0.4		–	0.4
Population size(P_s)	–	50	50	50
Max generations	–	100	100	100
Volatile factor(ρ)	–		0.2	0.2
Pheromones parameter(Q)	–		300	300
Crossover probability	–	0.85	–	–
Mutate probabolity	–	0.8	–	–

The cruising speed (V) of the aircraft is set to 600 kts and safety separation distance is 5 NM. At each 1 min time step (corresponding 10 NM in flight), each aircraft changes its heading based on information received from other aircraft. In our experiments, ρ and Q are set to 0.2 and 300, respectively. The results were collected and analyzed on the basis of 10 independent runs for each algorithm.

Appendix F Comparison results in the Classical Scenario

Besides, Figure F1 introduces graphics of these indices for the compared algorithms, with n from 1 to 28, where the values in each generation are averaged over 10 runs. Figure F1 provides a clear demonstration of their performance of them.

As shown in the Figure F1(a), the computational load of ant colony optimization and genetic algorithm are over 60s when 12 aircrafts are in conflict, thus not complying with requirements of real-time resolution. On the contrary, the computational load of the improved algorithm, which is slightly higher than the value of the artificial potential field method, can comply the real appicaiton requirements.

Figure F1(b) indicates that the artificial potential field method did not meet the feasibility requirement. The improved algorithm makes the aircraft only choose three flight directions, i.e. maintaining their original direction, and turning 30 degrees to the left and right, leading to feasible solutions. Furthermore, the proposed algorithm not only reduces the search

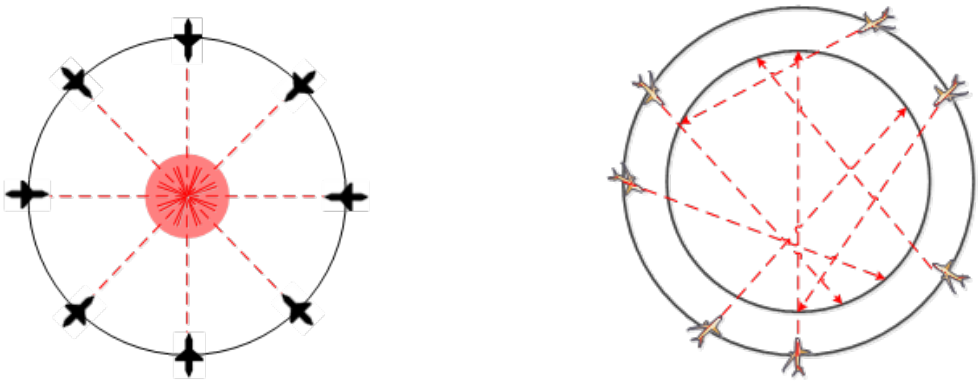

Figure E1 The classical scenario and random flight scenario

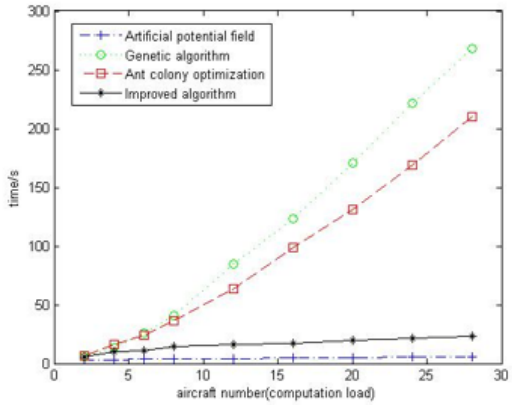

(a) Comparison of computational load for four algorithms

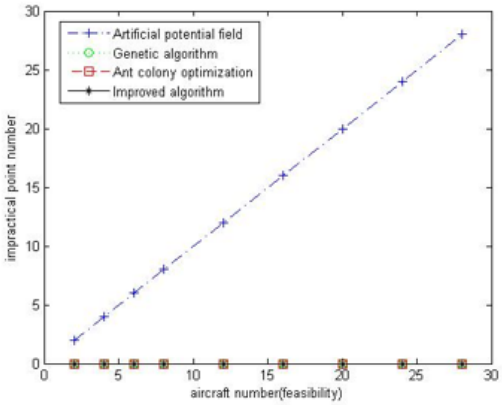

(b) Comparison of feasibility for four algorithms

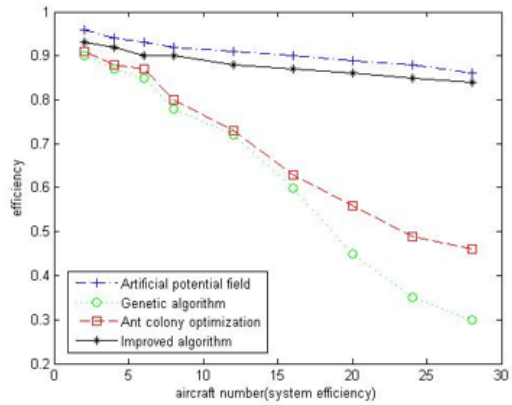

(c) Comparison of system efficiency for four algorithms

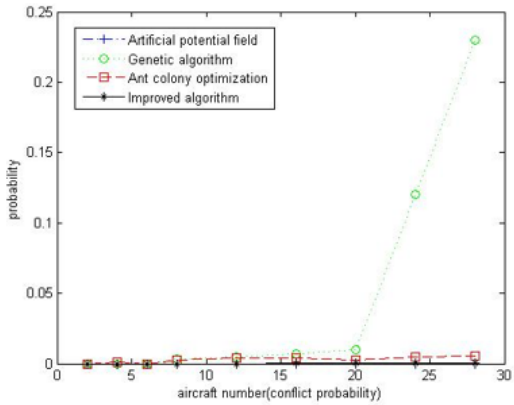

(d) Comparison of conflict probability for four algorithms

Figure F1 Comparisons for four algorithms in the Classical Scenario

space, but also can decrease the pilot's reaction time, which makes the implementation of the conflict resolution solution easier

It can be seen in the Figure F1(c), that the system efficiency of the improved algorithm is significantly higher than the ACO algorithm and GA,but lower than the artificial potential field algorithm. However, Figure F1(d) shows that the conflict probability of the ACO algorithm and GA are much higher than that of the artificial potential field algorithm and the improved algorithm.

From the experimental results, we can conclude that the artificial potential field algorithm has better performance in computational load, system efficiency and conflict probability, but performs unsatisfactorily in feasibility which causes algorithm unsuitable for the actual situation. The performance of the ACO and GA are also not satisfactory. Only the improved algorithm performs well in all four indices. Therefore, it complies with requirements of reliability, speed, safety and efficiency.

Appendix G Comparison results in the random scenario

This part of experiments aims to evaluate the efficiency of the improved algorithm in radical situation by comparing it with some existing algorithms.

A trajectory example of eight aircraft using the improved algorithm is shown in Figure G1. All aircraft go straight to the target position without conflict along their flight route.

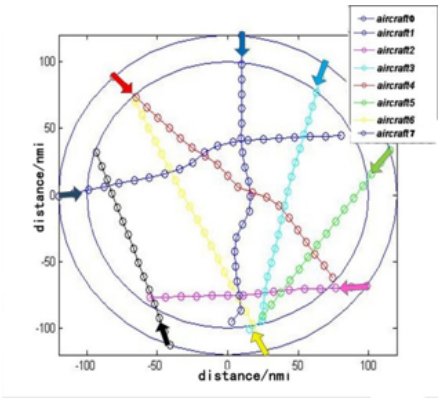

Figure G1 The results of aircraft conflict resolution by the improved algorithm

As in the first experiment, the results calculated based on 10 independent runs of the four algorithms in the random scenario are analyzed statistically in terms of their conflict probability, average computational load, feasibility, and system efficiency. The results are shown in Table G1. It also can be concluded that as the number of aircraft increases, the improved algorithm has the best performance. The overall tendency of the result is similar to that of the classic scenario. The improved algorithm behaves even better in the random flight scenario. The conflict probability, computation load and feasibility are all better than the result of the classic scenario.

Results of the compared algorithms in random scenario with n from 1 to 28 are also depicted in Figure G2, where the values in each generation are averaged over 10 runs. We can conclude that the improved algorithm meets the requirements of real-time application.

The reason why the hybrid algorithm performs the best is that it can take full advantages of the ACO algorithm and potential field method. The potential field method can get conflict-free trajectory in real time, but it may cause extremely unrealistic solution, such as the impractical heading change. On the other hand, the ACO algorithm can get near-optimal solution with high computation complexity which can satisfy the requirement of time. The improved algorithm uses the artificial potential field to obtain the initial high-quality conflict resolution paths to guide the optimization of ACO. The improved algorithm can reduce the searching space, improving the search capability. Hence, the hybrid algorithm can get the best solution effectively and efficiently in real time, and outperforms the existing approaches.

References

1 Zeghal K. A review of different approaches based on force fields for airborne conflict resolution; proceedings of the AIAA Guidance, navigation and control conference, F, 1998.
2 Archibald J K, Hill J C, Jepsen N A, Stirling W C, Frost R L, A satisficing approach to aircraft conflict resolution. IEEE Trans. Syst., Man, Cybern. C, Appl. Rev., 2008, 38(4):510C521.
3 Pallottino L, Feron E M, Bicchi A, Conflict resolution problems for air traffic management systems solved with mixed integer programming. IEEE Trans. Intell. Transp. Syst., 2002, 3(1):3C26 .
4 Kuchar J, Yang L, A review of conflict detection and resolution modeling methods. IEEE Trans. Intell. Transp. Syst., 2000, 1(4):179C189.

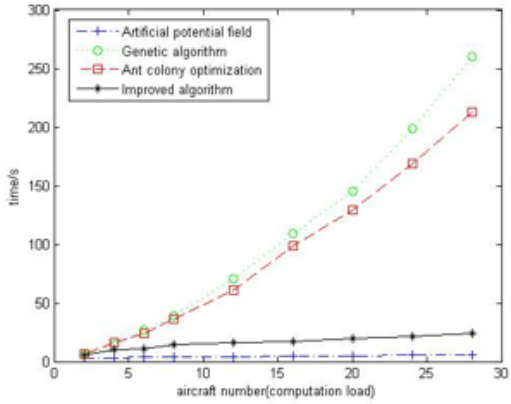

(a) Comparison of computational load for four algorithms

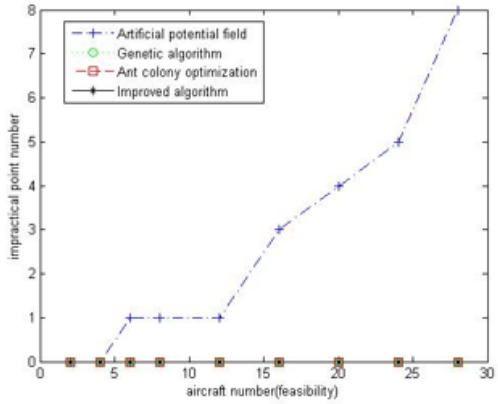

(b) Comparison of feasibility for four algorithms

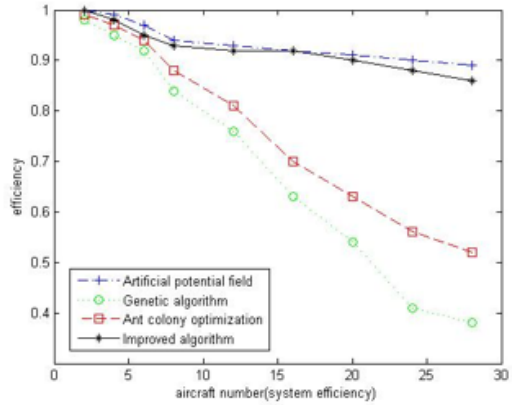

(c) Comparison of system efficiency for four algorithms

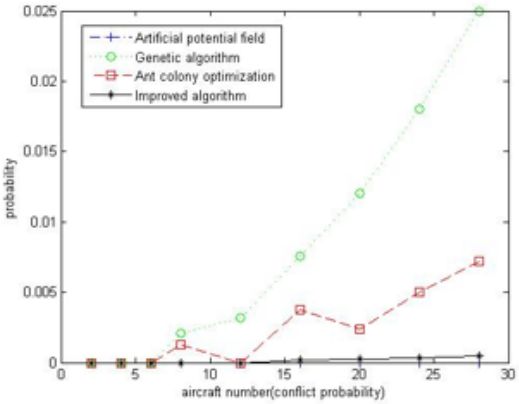

(d) Comparison of conflict probability for four algorithms

Figure G2 Comparisons for the four algorithms in the random flight scenario

Table G1 Comparisons of Artificial Potential Field, Ant colony optimization, and improved algorithm for the random flight scenario.(CL, F, SE and CP stand for the computational load, feasibility, system efficiency and conflict probability)

	ArtificialPotential Field				Genetic Algorithm				Ant Colony Optimization				Improved Algorithm			
Nub	CL(s)	F	SE	CP	CL(s)	F	SE	CP	CL(s)	F	SE	CP	CL(s)	F	SE	CP
1	2	3	4	5	6	7	8	9	10	11	12	13	14	15	16	17
2	3.2	0	1	0	5.6	0	0.98	0	6.2	0	0.99	0	6.1	0	1	0
4	3.4	0	0.99	0	14.7	0	0.95	0	15.9	0	0.97	0	10	0	0.98	0
6	3.6	1	0.97	0	26.8	0	0.92	0	24.3	0	0.94	0	11.1	0	0.95	0
8	3.9	1	0.94	0	39.2	0	0.84	0.0021	36.1	0	0.88	0.0013	14.9	0	0.93	0
12	4.2	1	0.93	0	70.2	0	0.76	0.0032	61.2	0	0.81	0	16.1	0	0.92	0
16	4.6	3	0.92	0	109.3	0	0.63	0.0076	98.4	0	0.7	0.0038	17.2	0	0.92	0.00015
20	5	4	0.91	0	145.3	0	0.54	0.012	129.6	0	0.63	0.0024	19.6	0	0.9	0.00024
24	5.5	5	0.9	0	198.4	0	0.41	0.018	169.2	0	0.56	0.005	21.7	0	0.88	0.00031
28	6.1	8	0.89	0	260.4	0	0.38	0.025	212.3	0	0.52	0.0072	23.7	0	0.86	0.00051

5 Alliot J M, Durand N, Granger G. Faces: a free flight autonomous and coordinated embarked solver; proceedings of the USA/Europe ATM R&D Seminar, F, 1998.